Hybrid Free Space Optical Communication and Radio Frequency MIMO System for Photonic Interference Separation

Taichu Shi, Yang Qi¹⁰, and Ben Wu¹⁰, Member, IEEE

Abstract—We propose and experimentally demonstrate a hybrid free space optical (FSO) communication and radio frequency (RF) multiple-input and multiple-output (MIMO) system for interference separation. The system switches between FSO and RF MIMO modes and makes use of the complementary advantages of the two modes. The MIMO receiver separates signal of interest from in-band interference with blind source separation (BSS), while the separation ratio is limited by the physical dimensions of the MIMO antenna array. With FSO channel, the system achieves over 30dB signal to interference plus noise ratio, so the wireless system can transmit signals with high orders of modulation. When the FSO channel is blocked and line-of-sight transmission condition is not satisfied, the system switches to the RF MIMO mode for interference cancellation. The wireless system maintains continuous transmission at a lower bit rate. Both the FSO mode and the RF MIMO mode can be seamless integrated with photonic signal processing system for wideband and real-time interference cancellation.

Index Terms—Interference cancellation, MIMO, free space optical communication.

I. Introduction

ADIO frequency (RF) spectrum is a scarce resource for wireless communications. Spectrum allocation methods use the spectral resource in an efficient way, so multiple systems share the same spectrum with the assigned bandwidths and time slots [1]. Such a sharing mechanism reaches its limit when all the spectra are well occupied, which leads to the interference management methods [2]. Multiple-input and multiple-output (MIMO) systems provide additional dimensions to support multiplexing [3], and enable the blind separation of interference from signal of interest (SOI), which allows many users to coexist with overlapped spectrum at the same time. Photonic blind source separation (BSS) has been demonstrated to process the MIMO signals and separate SOI from interferences [4]. By upconverting the mixed signals to optical frequencies, photonic BSS achieves GHz bandwidth in real-time [5], [6].

Beyond bandwidth, another factor that limits the coexistence of wireless systems is the separability of the mixed signals. Although signal separation has been explored in many algorithms, implementations of signal separation for

Manuscript received September 15, 2021; revised October 31, 2021; accepted December 27, 2021. Date of publication January 4, 2022; date of current version January 31, 2022. This work was supported by the National Science Foundation (NSF) under Grant ECCS-2128608. (Taichu Shi and Yang Qi contributed equally to this work.) (Corresponding author: Ben Wu.)

The authors are with the Department of Electrical and Computer Engineering, Rowan University, Glassboro, NJ 08028 USA (e-mail: wub@rowan.edu). Color versions of one or more figures in this letter are available at https://doi.org/10.1109/LPT.2022.3140364.

Digital Object Identifier 10.1109/LPT.2022.3140364

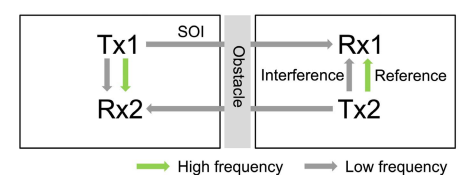


Fig. 1. Interference cancellation enabled by high frequency carriers (optical frequencies). The obstacle blocks the LOS transmission of high frequency signal, and low frequency signal can pass through the obstacle. (SOI: signal of interest).

the application of interference management meet with the physical challenges of the MIMO receivers. The dimension of the MIMO antenna array is a major factor that impact the capability of the system to separate the mixed signals [7]. With limited physical dimension, the antennas receive similar copies of the mixed signals, and thus interference cannot be completely separated from the SOI. Such case is called ill-condition, and widely exists in mobile receivers [8].

In this letter, we demonstrate a hybrid free space optical (FSO) and RF MIMO system for interference cancellation. The ill-condition problem is solved by sending a reference signal for interference cancellation through FSO channel. Since the reference signal only includes a copy of the interference signal, and channel coefficient of the FSO link is extremely different from that of the RF channel, the separation system achieves high signal to interference plus noise ratio (SINR). When line-of-sight (LOS) transmission is not available for the FSO channel, the system switches to RF MIMO mode to maintain continuous interference cancellation at a lower SINR. Mixed signals from both the FSO mode and RF mode are processed with the photonic BSS system for real-time signal processing.

FSO communication has been widely studied to expand the spectrum and transmission capacity of RF systems [9], [10]. Hybrid FSO/RF systems has been demonstrated to maximize the transmission rate by switching to optical frequencies when LOS is available [11], [12]. The hybrid FSO and RF MIMO system in this letter is different from the FSO communication systems that have been studied for high-speed transmissions [13], [14]. The FSO channel in this letter is to provide reference signal for interference cancellation in applications of long-distance RF wireless communications (e.g., Tx1-Rx1 in Fig. 1) and also passive RF receivers (e.g., radio telescope). The SOI carriers in such applications cannot switch to optical frequencies. Fig. 1 shows the schematic diagram of the interference model. Rx1 receives SOI from Tx1 and interference from Tx2.

1041-1135 © 2022 IEEE. Personal use is permitted, but republication/redistribution requires IEEE permission. See https://www.ieee.org/publications/rights/index.html for more information.

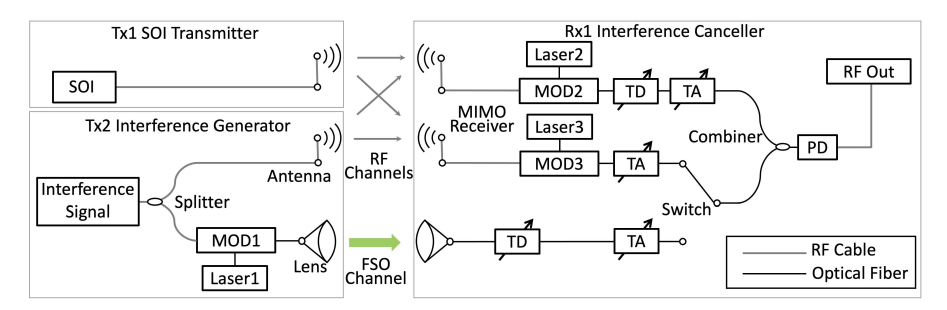


Fig. 2. Experimental setup of the interference cancellation system (MOD: Optical intensity modulators, FSO: free space optical communication, TD: optical tunable delay, TA: optical tunable attenuator/amplifier, PD: photodiode).

II. PRINCIPLE AND SYSTEM SETUP

A. Principle: Signal Separation With Ill-Condition

The separability of mixed signals is quantitatively described by the condition number of the mixing matrix. Consider the two Tx-Rx pairs shown in Fig. 1, the received signals from a MIMO receiver (Rx1) can be represented by:

$$X = AS$$
 or, $\begin{bmatrix} x_1 \\ x_2 \end{bmatrix} = \begin{bmatrix} a_{11} & a_{12} \\ a_{21} & a_{22} \end{bmatrix} \begin{bmatrix} s_{soi} \\ s_{int} \end{bmatrix}$ (1)

A is the mixing matrix. x_1 and x_2 are the received mixed signals from MIMO antennas. Separating SOI ssoi and interference s_{int} is to find the de-mixing matrix A^{-1} . The difficulty to accurately measure of de-mixing matrix is positively correlated to the condition number of the matrix A [15]:

$$cond(A) \equiv ||A|| \cdot ||A^{-1}||$$

$$||A|| \equiv \max_{j} \sum_{i=1}^{n} |a_{ij}|$$
(2)

$$||A|| \equiv \max_{i} \sum_{i=1}^{n} \left| a_{ij} \right| \tag{3}$$

The cases with large cond(A) are called ill-conditions [8]. A widely existing ill-condition is that each antenna of a MIMO device receives similar copies of both the interference and SOI $(x_1 \text{ is similar to } x_2 \text{ in Eq. 1})$. This problem happens when the receiving antennas are physically close to each other, and often exists in mobile devices, where the spatial dimensions between the antennas are limited. In the extreme condition, if the two receiving antennas receive the same copies of both SOI and interference, where $a_{11} = a_{21}$ and $a_{12} = a_{22}$, the condition number of the mixing matrix A is infinity, and SOI and interference cannot be separated.

The ill-condition problem can be effectively solved by sending a reference signal with the FSO channel. When the system is switched to the FSO mode, one of the MIMO antennas is replaced by the FSO link. The FSO link sends reference signals from the interference generator Tx2 to the receiver Rx1. The FSO reference signal only includes a copy of the interference signal, so the a_{21} in the mixing matrix is 0. Eq. 1 is changed to:

$$\begin{bmatrix} x_1 \\ x_2 \end{bmatrix} = \begin{bmatrix} a_{11} & a_{12} \\ 0 & a_{22} \end{bmatrix} \begin{bmatrix} s_{soi} \\ s_{int} \end{bmatrix}$$
 (4)

 a_{22} in Eq. 4 represents the FSO channel (Tx2-Rx1). a_{11} and a_{12} in Eq. 4 represent the RF channels (Tx1-Rx1 and Tx2-Rx1). Since the transmission property of the FSO channel is significantly different from the transmission property of the RF channel, a_{22} is significantly different from the a_{12} , which means Rx1 receives two different copies of interference.

 a_{11} is significantly different from the $a_{21}(a_{21} = 0)$, which means the receiver Rx1 receives two different copies of SOI. The ill-condition problem is solved.

B. Experimental Setup

Fig. 2 shows the experimental setup of the hybrid FSO and MIMO system. The system demonstrated functions of Tx1 SOI transmitter, Tx2 interference generator, and Rx1 interference canceller in Fig. 1. Rx1 can switch between FSO mode and RF MIMO mode and processes the mixed RF signals with photonic circuits in both modes. In FSO mode, the reference signal is intensity modulated on optical carrier with wavelength 1544nm (laser 1 in Fig. 2). The tunable delays and tunable attenuator/amplifiers at the receiver match the phases and amplitudes of interference and reference signals for interference cancellation. In the RF MIMO mode, the received RF signals are intensity modulated on laser 2 and laser 3 in Fig. 2. With photonic BSS, the de-mixing matrix is solved and implemented with tunable attenuator/amplifiers [4]. Fig. 3 demonstrates the relative positions of the antennas in the experiment. The setup includes two transmitting antennas (Tx1 and Tx2) and two receiving antennas (Rx1 MIMO receiver). Each antenna is represented by a black triangle (Fig. 3 (a)). All the four antennas are omnidirectional antennas with bandwidth up to 3GHz and peak frequency response at 800MHz. The relative positions of the antennas are drawn to scale in Fig. 3 (b). The two antennas at the origin (0,0) form a MIMO receiver, and the distance between the two antennas is 2cm. The distance between the SOI transmitter (Tx1) and the MIMO receiver (Rx1) is 111cm. The distance between the interference transmitter (Tx2) and the MIMO (Rx1) is 60cm, which is also the transmission distance of the FSO channel. The setup represents a general case for interference cancellation where interference transmitter is closer to receiver than the SOI transmitter.

III. RESULTS AND ANALYSIS

A. Mixing Matrix

The experimental results show that the condition number of the mixing matrix in the FSO mode is 5 times smaller than the condition number of the mixing matrix in the RF MIMO mode. Fig. 4 shows the magnitude of the mixing matrix in the RF MIMO mode. Because the physical locations of two antennas at the MIMO receiver are close, the two antennas receive very similar copies of the signals. Fig. 4 (a) shows that values of a_{11} and a_{21} are close to each other, which means the two antennas receive similar copies of SOI. Fig. 4 (b) shows that

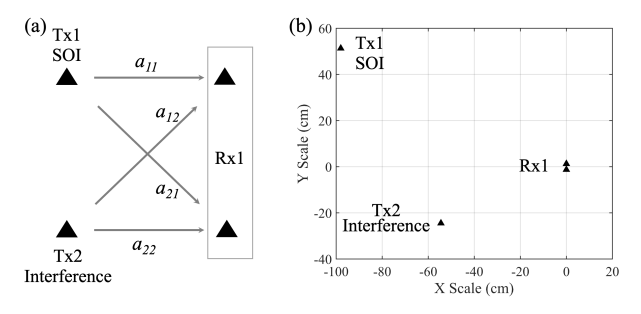


Fig. 3. (a) Schematic diagram for the mixing matrix. Each triangle shows a transmitting or a receiving antenna. (b) The actual positions of antennas in the experiment: Tx1 and Tx2 are two transmitting antennas for SOI and interference respectively; Rx1 includes two MIMO receiving antennas.

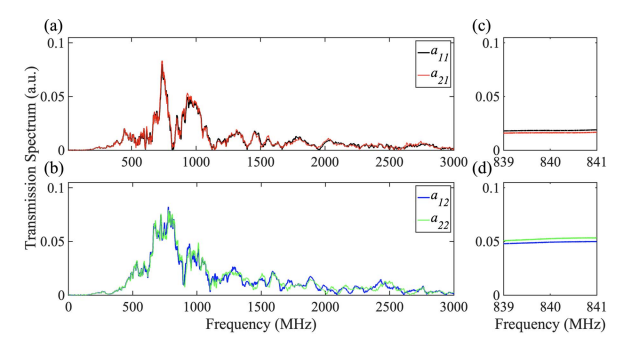


Fig. 4. Experimental measured mixing matrix when the system is in the RF MIMO mode (a) a_{11} and a_{21} (b) a_{12} and a_{22} (c) and (d) are the enlarged view at 840MHz.

the values a_{12} and a_{22} are close to each other, which means the two antennas receive similar copies of interference.

Figs. 4 (c) and (d) is the enlarged view of Figs. 4 (a) and (b) and show the frequency range used for both SOI and interference. The magnitude of the mixing matrix at 840MHz is:

$$A_{MIMO} = \begin{bmatrix} a_{11} & a_{12} \\ a_{21} & a_{22} \end{bmatrix} = \begin{bmatrix} 0.0184 & 0.0491 \\ 0.0162 & 0.0524 \end{bmatrix}$$
 (5)

The corresponding condition number is $cond(A_{MIMO}) = 41$. In the RF MIMO mode, the interference is separated from the SOI with BSS algorithm. When the receiver noise is close to the differential signals $(a_{11} - a_{21})s_{soi}$ and $(a_{21} - a_{22})s_{int}$, the BSS algorithm cannot accurately solve the de-mixing matrix, and which leads to ill-condition.

The ill-condition problem can be effectively solved by using a FSO channel to send the reference signal. The reference signal is sent from interference generator to the receiver, so it only includes a copy of interference, and does not include SOI. This means that a_{21} is zero at all the frequencies (Fig. 5 (a)). In the FSO mode, the switch in Fig. 2 is connected to the FSO channel. x_1 in Eq. 1 is from one of the MIMO antennas and x_2 is from the FSO channel. Since the frequency response of the FSO channel (green curve in Fig. 5 (b)) is significantly different from the frequency response of RF channel (blue curve in Fig. 5 (b)), a_{12} and a_{22} are significantly different in all the frequencies.

Figs. 5 (c) and (d) are the enlarged views of Figs. 5 (a) and (b), and the magnitude of the mixing matrix in the FSO mode is:

$$A_{FSO} = \begin{bmatrix} a_{11} & a_{12} \\ a_{21} & a_{22} \end{bmatrix} = \begin{bmatrix} 0.0184 & 0.0491 \\ 0 & 0.0826 \end{bmatrix}$$
 (6)

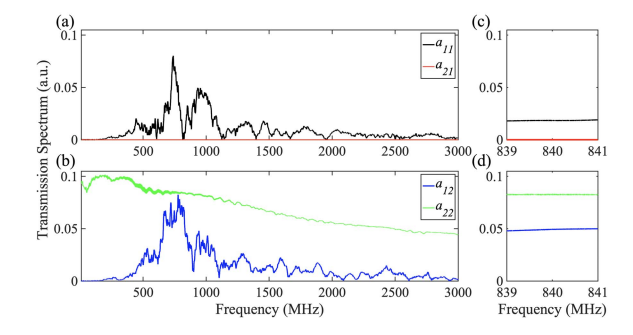


Fig. 5. Experimental measured mixing matrix when the system is in the FSO mode (a) a_{11} and a_{21} (b) a_{12} and a_{22} (c) and (d) are the enlarged view at 840MHz.

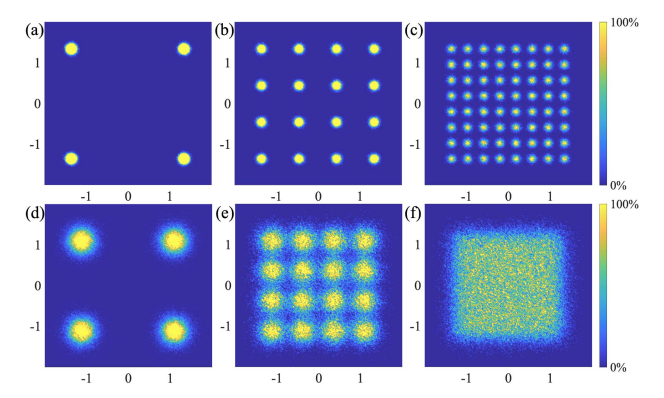


Fig. 6. Constellation diagrams of the recovered SOI. (a)-(c) FSO mode: modulation format of SOI is QPSK, 16QAM, 64QAM respectively; (d)-(e) RF MIMO mode: modulation format of SOI is QPSK, 16QAM, 64QAM respectively.

In the FSO mode, the condition number is cond (A_{FSO}) = 7, which is over 5 times smaller than the condition number of the RF MIMO mode. Since a_{11} is significantly different from a_{21} , and a_{12} is significantly different from a_{22} , the BSS system can calculate the de-mixing matrix orders of magnitude more accurately than the RF MIMO mode, which is demonstrated in the next section.

B. Recovered Signals

Fig. 6 shows the comparison of recovered SOIs between the FSO mode and RF MIMO mode. In the FSO mode (Figs. 6 (a)-(c)), the SINR is 33dB. Clear constellation diagrams are achieved for QPSK, 16QAM, and 64QAM modulations. In the RF MIMO mode (Figs. 6 (d)-(f)), since the system cannot accurately calculate the de-mixing matrix, the SOI and interference are not completely separated. The SINR is 15dB. The system can only operate with QPSK modulation (Fig. 6 (d)). With 16QAM, the recovered signals are noisy (Fig. 6 (e)). With 64QAM, the patterns of each point in the constellation diagram cannot be identified (Fig. 6 (f)).

Based on the results in Fig. 6, the receiver operates with FSO and RF MIMO modes alternatively for interference cancellation. When the LOS transmission is available, the receiver operates in FSO mode. The 33dB SINR enables high orders of modulation for SOI (16QAM and 64QAM). When the LOS transmission is not available, the receiver operates in RF MIMO mode to maintain the continuous interference cancellation, and the SOI deploys low order of modulation (QPSK).

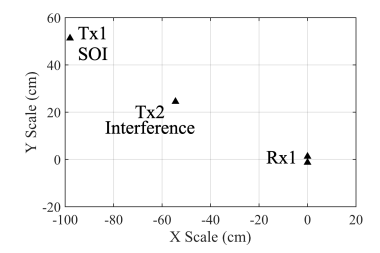


Fig. 7. The actual positions of antennas when SOI transmitter and interference transmitter are aligned with the receiver.

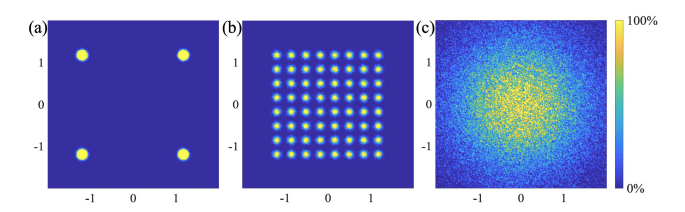


Fig. 8. Constellation diagrams of the recovered signals when SOI transmitter and interference transmitter are aligned. (a) System is in FSO mode and SOI is QPSK; (b) System is in FSO mode and SOI is 64QAM; (c) System is in RF MIMO mode and SOI is QPSK.

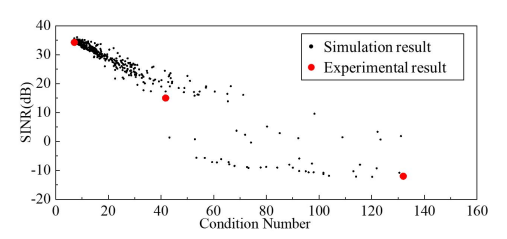


Fig. 9. SINR decreases with the increasement of the condition number.

To further compare the difference between the FSO mode and RF MIMO mode, the relative positions of Tx1, Tx2, and Rx1 are changed according to Fig. 7. In this case, Tx1 and Tx2 are on the same side of Rx1 and both of the transmitters are aligned with the receiver. Compared with Fig. 3 (b), this case is more challenging for the RF MIMO receiver to separate interference and SOI, and the mixing matrix is:

$$\mathbf{A} = \begin{bmatrix} a_{11} & a_{12} \\ a_{21} & a_{22} \end{bmatrix} = \begin{bmatrix} 0.0162 & 0.0491 \\ 0.0184 & 0.0524 \end{bmatrix} \tag{7}$$

The corresponding condition number is cond(A) = 132, which is about three times of the condition number in Eq. 5. In such case, the RF MIMO receiver is not able to separate interference with SOI and the received signal is pure Gaussian noise (Fig. 8 (c)). In the FSO mode, the mixing matrix is:

$$A = \begin{bmatrix} a_{11} & a_{12} \\ a_{21} & a_{22} \end{bmatrix} = \begin{bmatrix} 0.0162 & 0.0491 \\ 0 & 0.0826 \end{bmatrix}$$
 (8)

The corresponding condition number is cond(A) = 8, which close to the condition number in Eq. 6. The recovered SOIs in the FSO mode have clear constellation diagrams for both QPSK and 64QAM modulations with SINR 34dB (Figs. 8 (a) and (b)).

Fig. 9 shows the scatter plot of simulation results with 500 different mixing matrixes. The recovered SINR decreases with the increasement of condition number (black dots), which matches with the experimental results (red dots). The three red

dots from left to right correspond to the constellation diagrams of Fig. 6 (a), Fig. 6 (d) and Fig. 8 (c) respectively.

IV. CONCLUSION

We proposed and experimentally demonstrated a hybrid FSO and RF MIMO system for interference cancellation. The cancellation system switches between RF MIMO mode and FSO mode to takes advantage of the complementary benefits of the two modes. The MIMO receiver ensures the continuous interference cancellation and maintains the availability of the SOI channel when the FSO channel is blocked. When LOS transmission is satisfied, the system is switched to the FSO mode. The frequency response and transmission function of the FSO channel is significantly different from the RF channel, so BSS system in the FSO mode can solve the de-mixing matrix more accurately than the system in the RF MIMO mode. In the FSO mode, the system achieves 33dB SINR, so high orders of modulation, such as 16QAM and 64QAM can be applied for the SOI.

REFERENCES

- Y. Wang, Z. Ye, P. Wan, and J. Zhao, "A survey of dynamic spectrum allocation based on reinforcement learning algorithms in cognitive radio networks," *Artif. Intell. Rev.*, vol. 51, no. 3, pp. 493–506, Jun. 2018.
- [2] J. Yao et al., "Comprehensive study on MIMO-related interference management in WLANs," *IEEE Commun. Surveys Tuts.*, vol. 21, no. 3, pp. 2087–2110, 3rd Quart., 2019.
- [3] Y. L. Sit, B. Nuss, and T. Zwick, "On mutual interference cancellation in a MIMO OFDM multiuser radar-communication network," *IEEE Trans. Veh. Technol.*, vol. 67, no. 4, pp. 3339–3348, Apr. 2018.
- [4] A. N. Tait et al., "Demonstration of multivariate photonics: Blind dimensionality reduction with integrated photonics," J. Lightw. Technol., vol. 37, no. 24, pp. 5996–6006, Dec. 15, 2019.
- [5] P. Y. Ma, A. N. Tait, T. F. de Lima, C. Huang, B. J. Shastri, and P. R. Prucnal, "Photonic independent component analysis using an onchip microring weight bank," *Opt. Exp.*, vol. 28, no. 2, pp. 1827–1844, Jan. 2020.
- [6] J. J. Sun, M. P. Chang, and P. R. Prucnal, "Demonstration of over-the-air RF self-interference cancellation using an optical system," *IEEE Photon. Technol. Lett.*, vol. 29, pp. 397–400, Feb. 15, 2017.
- [7] R. T. Kobayashi, "Ordered MMSE-SIC via sorted QR decomposition in ill conditioned large-scale MIMO channels," *Telecommun. Syst.*, vol. 63, pp. 335–346, Oct. 2016.
- [8] H. L. Liu, "Blind separation of ill-condition mixed sources based on generalized eigenvalue," *Tien Tzu Hsueh Pao/Acta Electron. Sin.*, vol. 34, no. 11, pp. 2072–2075, Nov. 2006.
- [9] M. Z. Chowdhury, M. K. Hasan, M. Shahjalal, M. T. Hossan, and Y. M. Jang, "Optical wireless hybrid networks: Trends, opportunities, challenges, and research directions," *IEEE Commun. Surveys Tuts.*, vol. 22, no. 2, pp. 930–966, 2nd Quart., 2020.
- [10] R. Miglani and J. S. Malhotra, "Performance enhancement of high-capacity coherent DWDM free-space optical communication link using digital signal processing," *Photon. Netw. Commun.*, vol. 38, no. 3, pp. 326–342, Dec. 2019.
- [11] F. Nadeem, V. Kvicera, M. S. Awan, E. Leitgeb, S. S. Muhammad, and G. Kandus, "Weather effects on hybrid FSO/RF communication link," *IEEE J. Sel. Areas Commun.*, vol. 27, no. 9, pp. 1687–1697, Dec. 2009.
- [12] M. Usman, H.-C. Yang, and M.-S. Alouini, "Practical switching-based hybrid FSO/RF transmission and its performance analysis," *IEEE Pho*ton. J., vol. 6, no. 5, pp. 1–13, Oct. 2014.
- [13] A. Touati, A. Abdaoui, F. Touati, M. Uysal, and A. Bouallegue, "On the effects of combined atmospheric fading and misalignment on the hybrid FSO/RF transmission," *J. Opt. Commun. Netw.*, vol. 8, no. 10, pp. 715–725, Oct. 2016.
- [14] L. Huang et al., "Unified performance analysis of hybrid FSO/RF system with diversity combining," J. Lightw. Technol., vol. 38, no. 24, pp. 6788–6800, Dec. 15, 2020.
- [15] D. A. Belsley, E. Kuh, and R. E. Welsch, "The condition number," in Regression Diagnostics Identifying Influential Data Sources Collinearity. Hoboken, NJ, USA: Wiley, 2004, pp. 100–103.